Crossover from diffusive to tunneling regime in NbN-DyN-NbN ferromagnetic semiconductor tunnel junctions

P. K. Muduli, Avradeep Pal, Mark G. Blamire
*Department of Materials Science and Metallurgy,University of Cambridge, 27 Charles Babbage Road, Cambridge CB3 0FS,United Kingdom**
(Dated: March 6, 2014)

We have investigated NbN-DyN-NbN junctions with 1 to 10 nm thick DyN barriers. A crossover from diffusive (hopping) to tunneling-type transport was found in these junctions as the DyN thickness is reduced below ∼4 nm. We have also made a detailed study of magnetic and electrical properties of thicker DyN thin films deposited under similar condition; DyN films were found to be ferromagnetic with T_{Curie} ∼35 ± 5 K. Electrical transport of the junctions with ∼10 nm DyN was understood in terms of Shklovskii-Efros (SE)-type variable range hopping (VRH) at low temperature between 90 - 35 K. We estimated localization length ξ = 5.6 nm in this temperature range. Temperature dependence of resistance was found to deviate from SE-VRH below 35 K along with large suppression of resistance with magnetic field. This is correlated with onset of magnetism below 35 K. Large butterfly shaped MR up to ∼40% was found for the ∼10 nm thick DyN junction at 2 K. In the tunneling regime, barrier height of the tunnel junction was estimated ∼50 meV from Simmons model. Signatures of spin filtering was found in temperature dependence of resistance in tunnel junction with ∼3 nm thick DyN. Cooper pair tunneling in these junctions below T_C (∼10.8 K) of NbN was understood according to S-I-S tunneling current model. We found coherent tunneling of Cooper pairs through ∼1 nm thick DyN tunnel barrier with critical current I_C ∼12 μA. The critical current also showed modulation with magnetic field.

PACS numbers: 85.30.Mn, 75.76.+j,74.70.Ad,74.50.+r,72.25.Dc,

I. INTRODUCTION

Intrinsic ferromagnetic semiconductors have attracted great attention recently, as both the carrier density and magnetism can be manipulated by external stimuli. Ferromagnetic rare-earth nitrides (ReN) show semiconducting behavior with wide variety of optical, electronic and magnetic properties, which can be exploited for spintronics [1]. The most widely studied material in this class is GdN, which has a Curie temperature (T_{Curie}) around 70 K with a large magnetic moment of $7\mu_B/\mathrm{Gd}^{3+}$[2, 3]. Recently, spin-filtering with very large efficiency (∼70%) has been observed in tunnel junctions incorporating GdN as a tunnel barrier [4, 5]. Therefore, it is of interest to explore the electronic properties of other ferromagnetic ReNs. DyN is also a semiconducting ferromagnet with T_{Curie} ∼17-26 K [6]. The band gap of DyN varies from ∼0.91 to 2.9 eV in different reports [1, 7, 8]. Recently, Azeem *et al.* have reported an optical gap of ∼1.2 eV in polycrystalline DyN thin film[9]. Moreover the band gap in DyN is smaller compared to GdN. Therefore, one might expect smaller barrier height and hence higher conductance in tunnel junction made of DyN tunnel barrier compared to GdN.

To complicate matters, the nature of the magnetism and electrical properties of ReN is still under debate. It is widely accepted that the magnetism in ReN originates from large local spin magnetic moments on partially filled Re $4f$ shell which are coupled by indirect exchange interactions. Therefore, magnetism in these materials is a combination of localized and itinerant magnetic moments. Experimental results with DyN thin films for spintronics application have been limited so far: the only report is from Zhou *et al.*, where optical and magnetic property of DyN/GaN superlattice structures were investigated [10].

In this paper, we report the properties of tunnel junctions with DyN tunnel barriers. First, we present structural and magnetic properties of DyN thin films examined though x-ray diffraction and magnetization measurements. We then present detailed electrical transport studies of 7 μm × 7 μm junctions with different DyN barrier thickness. Diffusive type electrical transport in junctions with ∼10 nm thick DyN was examined with different bias voltage and magnetic fields. The barrier height of the tunnel junction was estimated from current-voltage (I-V) measurements above ferromagnetic transition temperature. Finally, quasiparticle tunneling through DyN has also been examined at different temperatures.

II. FABRICATION AND EXPERIMENTAL DETAILS

Reactive dc sputtering was used to deposit NbN-DyN-NbN trilayer films in an ultra-high vacuum (UHV) chamber. Residual oxygen and H_2O was minimized by baking the chamber for 12 hours which leads to a base pressure ∼2×10^{-9} mbar. Deposition was done at room temperature at 1.5 Pa with Ar-N_2 gas mixture of 8 % and 28 % for DyN and NbN, respectively. Low sputtering power

*Electronic address: pkm27@cam.ac.uk

~20 W was used for DyN, while higher sputtering power ~100 W was used for NbN. This is similar to the deposition condition we have used earlier for NbN-GdN-NbN tunnel junctions [4]. Films were deposited on 5 mm × 5 mm Si substrates capped with 250 nm of thermally oxidized SiO_2. A ~10 nm thick MgO buffer layer was deposited on all substrates which acts as an etch stop layer during fabrication of the tunnel junctions. The thickness of the top and bottom NbN was kept at 50 nm in all cases, while the DyN thickness was varied from ~1-10 nm. Tunnel junctions were fabricated from the trilayers using a mesa process involving optical lithography, Ar-ion and CF_4 plasma etching. For structural and magnetic characterization, thicker DyN films sandwiched between ~7 nm thick AlN protective layers were prepared under similar conditions. Magnetization measurements were performed in a vibrating sample magnetometer (VSM) from Cryogenic Limited. Crystallographic structure of the films was examined by the x-ray diffraction (XRD) measurements.

III. RESULTS

A. Structural and magnetic properties of DyN thin film

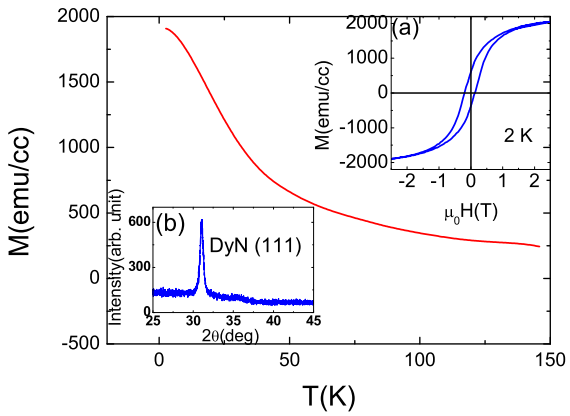

FIG. 1: (Color online) Temperature dependence of field-cooled (FC) magnetization of a ~100 nm thick DyN thin film. Magnetization was measured with 2.5 T magnetic field applied in the plane of the film. Magnetic hysteresis loop measured at 2 K is shown in inset(a). X-ray diffraction pattern of a 200 nm thick film is shown in inset (b).

Similar to other rare earth metal nitrides, DyN crystallizes in a FCC rock-salt structure. To understand the crystallographic structure of the films, we performed XRD measurements of thicker films deposited under similar conditions used for the junctions. A θ-2θ diffraction pattern of a ~200 nm thick film with ~7 nm AlN capping layer is shown in the inset (b) of Fig. 1. An intense peak at 2θ = 31.06 can be observed. This is close to 2θ = 31.589 which corresponds to (111) reflection of DyN as per JCPDS file no 15-0884. The films are, therefore, fairly textured. A strong (111) reflection is also found in GdN films deposited under similar conditions[11].

To avoid the strong diamagnetic moment of superconducting NbN at low temperature, films with AlN capping were also used for magnetization measurements. Fig. 1 shows the temperature dependence of magnetization of a ~100 nm thick DyN film. As temperature was decreased magnetization was found to increase with tendency towards saturation below 5 K. A Curie temperature (T_C) of ~35 K ± 5 K was found from Arrott plot method (see supplementary). This is slightly higher than the value (T_C ~17-26 K) reported in literature for bulk and thin films of DyN [6, 7, 8, 12]. Field-dependent magnetization measured at 2 K is shown in inset (a) of Fig. 1. We found a small asymmetry in the hysteresis loop with H_{C+} = 0.123 T and H_{C-} = -0.203 T. The coercive field ($H_C = (H_{C+} + H_{C-})/2$) was found to be ~0.16 T; this is much larger compared to ferromagnetic GdN films grown under similar conditions (H_C ~0.005 T)[11]. The asymmetry might be result of a presence of a antiferromagnetic phase along with dominant ferromagnetic phase similar to GdN thin films[11]. The magnetization is found to saturate above 2 T.

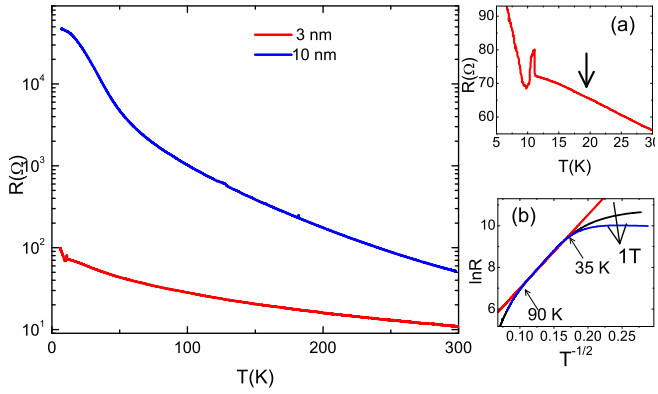

FIG. 2: (Color online) Temperature dependence of resistance of the junctions with ~10 nm (blue) and ~3 nm (red) DyN. (a) Zoomed-up view between 4-30 K for the junction with 3 nm thick DyN. (b) Plot of lnR vs. $T^{-1/2}$ for the 10 nm thick DyN junction with 0 and 1 T magnetic field. Straight line between 35- 90 K shows SE-VRH model fitting. Deviations from the SE-VRH model can be seen below ~35 K.

B. Electrical transport properties of NbN-DyN-NbN devices

Fig. 2 shows the temperature dependence of the resistance $R(T)$ of junctions with 10 and 3 nm thick DyN.

Both the junctions showed a semiconductor-type temperature dependence with deviations at low temperature. However, three order of magnitude difference in resistance can be seen for the two films. As discussed later, junctions with 10 and 3 nm thick DyN can be understood in a diffusive and tunnelling regime, respectively. As NbN becomes superconducting below ∼10.8 K, a change in slope can be observed in $R(T)$ of 10 nm DyN junction below this temperature. For junction with 3 nm DyN a clear drop in resistance can be observed below this temperature. A plot of temperature dependent resistance for the 3 nm thick DyN junction in the range 5 to 30 K is shown in Fig. 2(a). The decrease in slope below 25 K is probably due to onset of spin-filtering.

Electrical transport in the ∼10 nm junction can be understood in terms of variable range hopping under the influence of a Coulomb interaction. Recently, Pinto *et al.* have shown that in ferromagnetic GaGdN films, the temperature dependence of resistivity for higher temperatures can be explained by Mott variable range hopping whereas, at low temperatures, transport is dominated mostly by Shklovskii-Efros (SE)-type variable range hopping [13]. We found that at low temperatures SE-type variable range hopping (SE-VRH) describes our temperature dependence of resistivity data very well. According to SE-VRH resistance can be written as[14];

$$\mathrm{R} = \mathrm{R}_0 \exp(T_{SE}/T)^{1/2} \tag{1}$$

where $T_{SE} = \frac{\beta e^2}{4\pi\epsilon_0\kappa k_B \xi}$, κ is the macroscopic dielectric constant, $\beta = 2.8$, k_B is Boltzmann's constant and ξ is the localization length. Figure 2(b) shows a plot of lnR vs. $T^{-1/2}$ in the temperature range 11- 250 K. Between 90 and 35 K, $lnR \propto T^{-1/2}$ and the slope gives $T_{SE} =$ 1255.67 K. Considering, $\kappa = 6.57$ [1], we found $\xi = 5.6$ nm. Below 25 K, as magnetism sets in, the temperature dependence of the resistance was found to deviate from SE-VRH-type model. The deviation was found to increase with increasing magnetic field as shown in Fig. 2(b). As magnetism in rare earth nitrides is mediated by carriers, different type of hopping mechanism can be invoked to understand the electrical transport in the ferromagnetic phase.

Fig. 3 shows the temperature dependence of the magneroresistance (MR), defined as $MR = (R(H) - R(0))/R(0)$, for a 10 nm thick DyN junction. Clear butterfly-shape loop magnetoresistance up to 40% at 2 K was found even for a small field of 0.5 T. The MR was found to reduce significantly (∼20%) as the temperature is increased to 20 K. $R(T)$ measurements for magnetic field $H = 0$ and 1 T is shown in the inset. Significant MR can be observed up to ∼35 K. One can note here that in GdN thin films, the temperature dependence of resistivity shows an anomalous peak at T_C and resistivity falls an order of magnitude in the ferromagnetic phase. MR up to 35% has been found near T_C in epitaxial GdN films with magnetic field ∼4 T[15, 16].

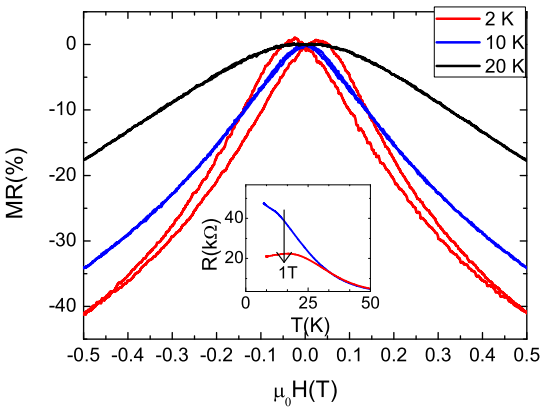

FIG. 3: (Color online)MR ($MR = (R(H) - R(0))/R(0)$) as a function of magnetic field and temperature for a ∼10 nm thick DyN junction. Inset shows large suppression of resistance with magnetic field ∼1 T.

IV. DISCUSSION

A. Tunneling Property of DyN tunnel barrier

Devices with DyN thickness ∼4 nm or less showed a strongly non-linear I-V similar to tunneling through a rectangular barrier, when measured above T_C (∼10.8 K) of NbN. Below 10.8 K, a clear superconducting gap structure appeared in the I-V curves indicating electrical transport is mainly due to elastic tunneling. Therefore, electrical transport in these junctions is dominated by tunneling process. The effective barrier height ϕ can be calculated from simple rectangular tunnel barrier model of Simmons[17]; fitting was performed on IV curves measured at 40 K, to avoid any complication due to exchange splitting of the barrier height below ferromagnetic transition of DyN. Barrier heights of junctions for different thickness of DyN are shown in the inset of the Fig. 4(b). Although, the bulk DyN has band gap ∼910 meV [1], much smaller barrier heights measured in these experiments seem to be a consistent feature of ReN barriers. For tunnel junctions with GdN the barrier height has been estimated to be ϕ ∼100 meV, whereas the band gap is as large as ∼980 meV [1, 5].

Fig. 4(a) shows I-V and $dI/dV - V$ curve of a junction with 2 nm thick DyN barrier measured at 4.2 K. A clear superconducting gap can be seen. The quasiparticle tunneling conductivity $G(V) = dI/dV$ in a S-I-S junction can be written as;

$$\frac{G_s(V)}{G_N(V)} = \frac{d}{d(eV)} \int_{-\infty}^{\infty} N(E+eV)N(E)[f(E) - f(E+eV)]dE + \frac{V}{R_{sh}} \tag{2}$$

Where $N(E)$ is density of states and $f(E)$ is Fermi distribution function. Here R_{sh} is a shunt resis-

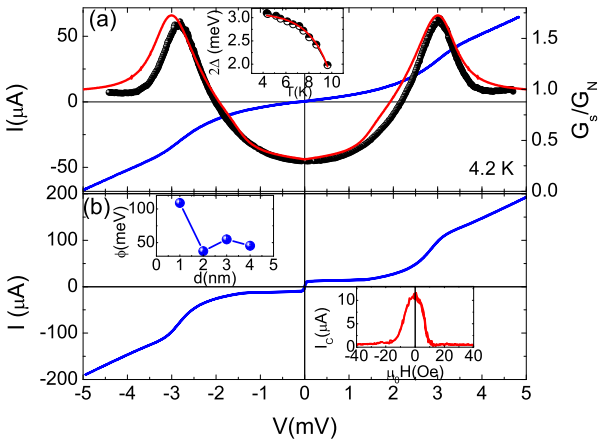

FIG. 4: (Color online)(a) IV curve along with normalized $dI/dV - V$ of a junction with ∼3 nm DyN measured at 4.2 K. Solid red line is a fit to the model described in the text with fitting parameter $2\Delta = 3.1$ meV and $\Gamma = 0.165$. Inset shows the temperature dependence of superconducting gap 2Δ. The solid red line is a fit to BCS type temperature dependence. (b) IV curve of a tunnel junction with 1 nm DyN measured at 4.2 K. Upper inset shows barrier height for different thickness of DyN extracted from fitting Simmons model to IV curves measured at 40 K. Bottom inset shows modulation of critical current I_C with magnetic field

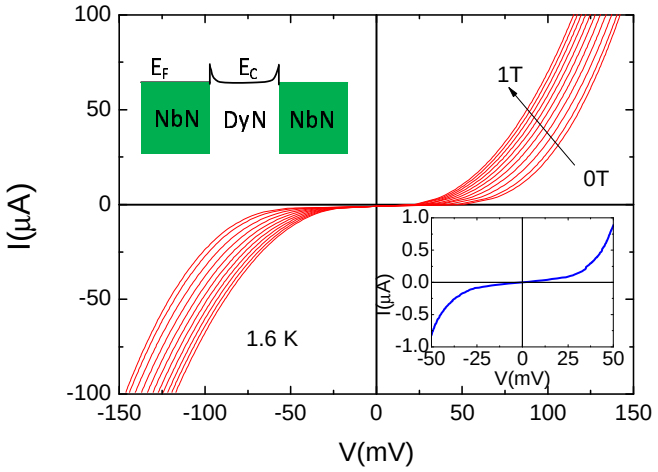

FIG. 5: (Color online) I-V curves of 10 nm DyN device measured at 1.6 K with different magnetic fields up to 1 T. Upper inset shows potential profile of a double Schottky barrier for this junction. Here E_F is the Fermi energy of NbN and E_C is the conduction band edge of DyN. I-V plot for lower voltages 50 mV is shown in lower inset.

tance in series with the S-I-S junction. Conductivity $G(V)$ can be calculated numerically by integrating Eq. (2) with a modified density of states, $N(E) = N(0)\left|\mathrm{Re}\left(\frac{E/\Delta - i\Gamma}{\sqrt{(E/\Delta - i\Gamma)^2 - 1}}\right)\right|$. Here Δ is the superconducting gap and Γ is the smearing parameter. Solid line in Fig. 4(a) shows calculated $G(V)$ from Eq. (2) with $2\Delta = 3.1$ meV and $\Gamma = 0.165$. Inset in Fig. 4(a) shows the superconducting gap 2Δ extracted from $dI/dV - V$ curves measured at different temperatures. Solid lines are fit to BCS type temperature dependence, $\Delta(T) = \Delta(0)\tanh(2.2\sqrt{(T_C - T)/T})$, with $2\Delta(0) = 3.07$ meV and $T_C = 10.74$ K.

Junctions with ∼1 nm DyN showed Josephson junction like behavior with a small critical current I_C ∼12 μA as shown in Fig. 4(b). The magnetic field dependence of I_C is shown in the inset of Fig. 4(b). A clear modulation of I_C similar to Fraunhofer-like oscillation can be observed.

B. Electrical transport in non-tunneling regime

To understand the electrical transport of ∼10 nm DyN junctions in the ferromagnetic phase in more detail, we performed I-V measurements at 1.6 K with different magnetic fields. Fig. 4 shows I-V curves between ±150 mV for magnetic fields H up to 1 T with a step of 0.1 T. We could not find any superconducting band structure in I-V curves for these junctions. I-V curves measured at lower voltages is shown in the lower inset of Fig. 4. Similar nonlinear I-V with no superconducting gap was also found for all junctions with DyN thickness ≥4 nm. We found that Simmons rectangular tunnel barrier model does not fit to these non-linear IV curves. Due to large conductivity mismatch between DyN and NbN, Schottky barrier is expected at the interface between DyN and NbN[5, 18]. The resulting Schottky contact at the two interfaces forms two triangular shaped Schottky barriers with narrow depletion width. The potential profile of such double Schottky barrier is shown in the upper inset of Fig. 5. However, a quantitative estimation of Schottky barrier height is difficult due to the large exchange splitting of the DyN below T_C. Attempts to fit I-V curves with standard Schottky barrier equations yielded ideality factors much greater than 1, indicating a process other than thermionic emission also contributes to the total current through these junctions. In the thick ∼10 nm DyN junction electrical transport is mostly dominated by thermionic emission across the Schottky barrier along with normal diffusive transport. As the thickness of the DyN is decreased direct tunneling starts to dominate across the barrier. The crossover from the diffusive (hopping) to complete tunneling type electrical transport was found for DyN thickness <4 nm where a clear superconducting gap structure can be seen in the I-V curves measured below T_C of NbN.

The behavior of I-V curves (shown in Fig. 5) in the higher voltage ($> \pm 75$ mV) region can be explained by an activationless hopping model. At sufficiently high electric field (or applied voltage) the film resistance becomes temperature independent. Electrical transport in this regime is mostly dominated by hopping due to applied electric field. In this activation less hopping regime, the current-

voltage characteristics is given by[19, 20, 21];

$$\mathrm{I} = \mathrm{I}_0 \exp(-V_0/V)^{1/2} \quad (3)$$

where, $V_0 = \frac{k_B T_0}{e\xi}$ and ξ is localization length. Here T_0 is a characteristic temperature related to localization length as $T_0 \propto 1/\xi$.

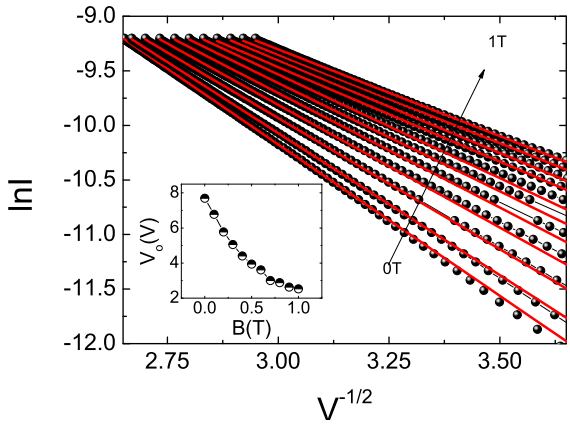

FIG. 6: (Color online)Plot of lnI vs. $V^{-1/2}$ for the 10 nm thick DyN film at different magnetic fields. Straight line fits (red) are between 75-150 mV. Inset shows V_0 as a function of magnetic field

Fig. 6 shows a plot of lnI vs $V^{-1/2}$ at different magnetic fields. A clear linear dependence between lnI and $V^{-1/2}$ can be observed at higher voltages between 75-150 mV. From the slope of the linear fits, V_0 was calculated and plotted in the inset of Fig. 6. Given that$V_0 \propto 1/\xi^2$, localization length ξ is found to increase with magnetic field. In presence of a magnetic field the amplitude and phase of wave function of the hopping electron might alter. This can give rise to larger localization length along with decrease in resistance.

V. CONCLUSIONS

In conclusion, we have presented a detailed study of the electrical and magnetic property of DyN thin films along with NbN-DyN-NbN tunnel junctions. DyN films were found to be magnetic with ferromagnetic Curie temperature T_C ∼35 K. In the range 90-35 K, temperature dependence of resistance of junction with ∼10 nm DyN was analyzed using SE-VRH type model. Localization length ξ ∼5.6 nm was estimated from this. Large magnetoresistance ∼40% was found at 2 K in this junction even for a small magnetic field ∼0.5 T. Junctions with DyN thickness ∼4 nm or less showed tunneling behavior with clear superconducting gap in I-V and dI/dV measurements. Signatures of spin filtering was found for junction with ∼3 nm DyN. Quasi-particle tunneling through DyN was understood in terms of a S-I-S tunneling model. For 1 nm thick DyN junction Jospeshon like behavior was found with critical current I_C ∼12 μA, which also showed modulation with magnetic field. However, NbN-DyN-NbN junctions were found to be more resistive compared to NbN-GdN-NbN junctions of comparable thickness reported by us earlier[5]. As electrical and magnetic property of DyN is very sensitive to different level of N vacancy, different deposition conditions of DyN can be explored to optimize the magnetization and resistivity of NbN-DyN-NbN junctions.

Acknowledgments

This work was supported by the ERC Advanced Investigator Grant SUPERSPIN. Authors thank Dr K. Senapati for useful discussions and Dr David Gustafsson for proof reading the manuscript.

[1] F. Natali, B. J. Ruck, N. O. V. Plank, and H. J. Trodahl,S. Granville, C. Meyer and W. R. L. Lambrecht, Progress in Materials Science **58**, 1316 (2013).
[2] G. Busch, J. Appl. Phys. **38**, 1386 (1967).
[3] D. P. Schumacher and W. E. Wallace, J. Appl. Phys. **36**, 984 (1965).
[4] K. Senapati, M. G. Blamire, and Z. H. Barber, Nature Materials **10**, 849 (2011).
[5] Avradeep Pal, K. Senapati, Z. H. Barber, M. G. Blamire, Adv. Mater. **25**, 5581 (2013).
[6] O. Vogt and K. Mattenberger, in *Handbook on the Physics and Chemistry of Rare Earths*, Vol. 17, edited by K. A. Gschneidner, L. Eyring, G. H. Lander, and G. R.Choppin (Elsevier, Amsterdam, 1993) pp. 301-407.
[7] F. Hulliger, *Handbook on the Physics and Chemistry of Rare Earths*, Vol. 4, edited by K. A. Gschneidner and L. Eyring (Elsevier, Amsterdam, 1979) pp. 153-236.
[8] A. R. H. Preston, S. Granville, D. H. Housden, B. Ludbrook, B. J. Ruck, H. J. Trodahl, A. Bittar, G. V. M. Williams, J. E. Downes, A. DeMasi, Y. Zhang, K. E. Smith, and W. R. L. Lambrecht, Phys. Rev. B **76**, 245120 (2007).
[9] M. Azeem,B. J. Ruck, Binh Do Le, H. Warring, H. J. Trodahl, N. M. Strickland, A. Koo, V. Goian and S. Kamba, J. Appl. Phys. **113**, 203509 (2013).
[10] Y. K. Zhou, M. S. Kim,N. Teraguchi, A. Suzuki, Y. Nanishi, H. Asahi, Phys. Status Solidi B **240** , 440 (2003).
[11] Kartik Senapati, Thomas Fix, Mary E. Vickers, Mark G. Blamire, and Zoe H. Barber, Phys. Rev. B. **83**, 014403 (2011).
[12] N. Sclar,J. Appl. Phys. 35, 1534 (1964).
[13] A. Bedoya-Pinto, J. Malindretos, M. Roever, D. D. Mai,

and A. Rizzi, Phys. Rev. B. **80**, 195208 (2009).
[14] B. I. Shklovskii and A. L. Efros, *Electronic Properties of Doped Semiconductor*(Springer, Berlin, 1984).
[15] B. M. Ludbrook, I. L. Farrell, M. Kuebel, B. J. Ruck, A. R. H. Preston, H. J. Trodahl, L. Ranno, R. J. Reeves, and S. M. Durbin, J. Appl. Phys. **106**, 063910 (2009).
[16] F. Leuenberger, A. Parge, W. Felsch, K. Fauth, and M. Hessler, Phys. Rev. B **72**, 014427 (2005).
[17] J. G. Simmons, J. Appl. Phys. **34**, 1793 (1963).
[18] M. Mehbod, W. Thijs, and Y. Bruynseraede, Phys. Status Solidi A **32**, 203 (1975).
[19] D. Yu, C. Wang, B. L. Wehrenberg, and P. Guyot-Sionnest, Phys. Rev. Lett. **92**, 216802 (2004).
[20] S. M. Grannan, A. E. Lange, E. E. Haller, and J. W. Beeman, Phys. Rev. B **45**, 4516 (1992).
[21] F. Tremblay, M. Pepper, D. Ritchie, D. Peacock, J. Frost, G. Jones and G. Hill, Phys. Rev. B **40**, 3387 (1989).